Generating novel focal patterns for a radial variant vector beam focusing through a dielectric interface

Lavanya Maruthasalam[1], Duraisamy Thiruarul[2], Karuppaiya Balasundaram Rajesh[2*], Zbigniew Jaroszewicz[3]

[1]*Department of Physics, PSGR Krishnammal College for Women, Coimbatore, Tamilnadu, India, 641004*
[2]*Department of Physics, Chikkanna Government Arts College, Tiruppur, Tamilnadu, India*
[3]*Institute of Applied Optics, Department of Physical Optics, Warsaw, Poland*

Received February 21, 2023; accepted March 31, 2023; published March 31, 2023

Abstract— Electric and magnetic energy densities as well as energy flux (Poynting vector) for a radial variant vector beam focusing through a dielectric interface is analyzed numerically based on vector diffraction theory. Electric and magnetic energy densities are tailored by properly manipulating radial as well as initial phases to generate novel focal patterns in the focal area. These peculiar properties may find application in fields such as optical trapping, optical recording, magnetic recording, magnetic resonance microscopy and semiconductor inspection.

In recent years, tight focusing of a laser beam with different states of polarization (SoP) has attracted intensive attention and extensive investigation, because of their fascinating features and wide potential applications [1–5]. Additional amplitude and phase filters in the input pupil demonstrated the generation of novel focal structures such as a sharper focus, optical needle, multiple focal spots/holes, flat-top profile, optical chain, optical cage, focal spot arrays etc. [6–8]. However, these filters greatly affect the strength of the input beam, and the alignment of such filters is very complicated and tedious. On the other hand, these novel focal patterns can also be demonstrated by utilizing the intrinsic degree of freedom of polarization of an input beam without any additional phase or amplitude filters. Recently, radially variant vector beams have been numerically explained and experimentally generated [9–11]. More recently, Zhongsheng Man *et al*. numerically have studied the focusing properties of a radial variant vector beam [12–14]. Most of the previous cases, only concentrate on the focal properties of electric field distribution in the focal plane. As a counterpart, demonstration of both the magnetic field distribution as well as the Poynting vector distribution (energy flux) in the focal plane, are of great interest in optical trapping experiment. On the other hand, Kotlyar et al report so many articles based on energy flux in the reverse direction [15–17]. Moreover, in some practical applications such as optical trapping and semiconductor inspection, the laser beam focusing through the media of different refractive indices are mentioned [18]. Based on the Richard and Wolf formulas, Török *et al*. obtained explicit expression for laser beam through a dielectric interface [19–20]. Z. Zhou *et al*. studied tight focusing properties of high-order axially symmetric polarized beams through a dielectric interface and calculated the electric and magnetic field intensity distribution in the focal plane [21]. Recently, many reports have explained focusing through a dielectric interface with different amplitude and polarization distribution [22–23]. In this paper, based on the Richards and Wolf vector diffraction theory, there are analyzed numerically the properties of electric and magnetic fields as well as energy flux for tightly focused polarized beams with arbitrary geometric configurations of linear polarization through a dielectric interface.

Figure 1 shows the schematic diagram of a focusing system. A radially variant vector beam is focused from air (medium 1) on to silicon (medium 2). Here *d* is the distance between the interface and geometrical focus.

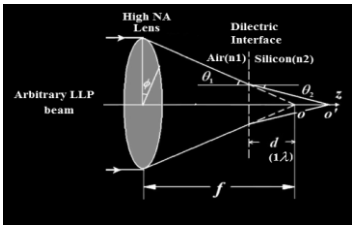

Fig.1. Scheme of a focusing system.

The electric and magnetic energy densities in the cylindrical coordinate system (r, ϕ, z) are given by [24]:

$$E(r,\psi,z) = \frac{-iC}{2}\int_0^{\alpha}\int_0^{2\pi} \sin\theta_1 \sqrt{\cos\theta_1}\, A(\theta_1,\phi)\, exp[ik_o(\Phi)]$$
$$exp[ik_2 z\cos\theta_2 + ik_1 r\sin\theta_1\cos(\phi-\psi)]E_e d\phi d\theta_1,$$

$$H(r,\psi,z) = \frac{-iC}{2}\int_0^{\alpha}\int_0^{2\pi} \sin\theta_1 \sqrt{\cos\theta_1}\, A(\theta_1,\phi)$$
$$exp[ik_o(\Phi)]\, exp[ik_2 z\cos\theta_2 + ik_1 r\sin\theta_1\cos(\phi-\psi)]H_m d\phi d\theta_1,$$

where C is the constant, α = $\sin^{-1}$(NA) is the maximal angle determined by the NA of the objective; $A(\theta_1, \phi)$ is the relative amplitude of the incident beam, which is considered as unity in over calculation. E_e and M_m are the

* E-mail: rajeskb@gmail.com

 © 2023 Photonics Society of Poland

electric and magnetic vectors in the focus and are expressed as [21]:

$$E_e = \begin{bmatrix} E_{er} \\ E_{e\phi} \\ E_{ez} \end{bmatrix} = \begin{bmatrix} cos(\delta-\phi)\cos\theta_2 \cos(\phi-\psi)t_p + sin(\delta-\phi)sin(\psi-\phi)t_s \\ cos(\delta-\phi)\cos\theta_2 sin(\phi-\psi)t_p + sin(\delta-\phi)cos(\psi-\phi)t_s \\ -\cos(\delta-\phi)\sin\theta_2\, t_p \end{bmatrix},$$

$$M_m = \begin{bmatrix} M_{mr} \\ M_{m\phi} \\ M_{mz} \end{bmatrix} = \begin{bmatrix} cos(\delta-\phi)sin(\psi-\phi)t_p - sin(\delta-\phi)\cos\theta_2 \cos(\phi-\psi)t_s \\ cos(\delta-\phi)\cos(\psi-\phi)t_p - sin(\delta-\phi)\cos\theta_2 sin(\phi-\psi)t_s \\ sin(\delta-\phi)\sin\theta_2\, t_s \end{bmatrix}$$

$$\delta = b\left(\frac{2\pi \sin\theta_1}{\sin\alpha}\right) + c,$$

with azimuthal and radial index, respectively and c is the initial phase and where ϕ is the aberration function of the dielectric medium and t_p and t_s are the Fresnel amplitude transmission coefficients for parallel and perpendicular polarization states, respectively, which are given by:

$$t_s = \frac{2\sin\theta_2\cos\theta_1}{sin(\theta_1+\theta_2)}; \quad t_p = \frac{2\sin\theta_2\cos\theta_1}{sin(\theta_1+\theta_2)\cos(\theta_1-\theta_2)};$$

$$\Phi = kd(n_2\cos\theta_2 - n_1\cos\theta_1).$$

The Poynting vector distribution in the focal plane in terms of electric and magnetic field is expressed as [24]:

$$S \sim \frac{c}{8\pi} Re(E \times H^*),$$

where the asterisk denotes the complex conjugation of a magnetic field. The other parameters are fixed as NA = 0.95, n_1 =1, n_1 =3.5, λ = 1λ , d = 1λ.

Figure 2 shows the electric and magnetic field intensity distribution both in the focal plane and through focus with corresponding Poynting vector distribution with b = 0.1. Specifically, Fig. 2(a) shows a small radial change in the input beam structure due to the radial index value b = 0.1. The electric field through focus got three intensity peaks (Fig. 2(h)), the central peak dominated by E_ϕ component at the same time two side peaks dominated by E_r component, respectively. The corresponding magnetic field shows an axially extended focal spot with FWHM of (1λ) and DOF of (15λ), described in Fig. 2(k–m). The transverse component of Poynting vectors is the same as in the previous case but the longitudinal component of the Poynting vector shows a longitudinal energy flow at the focus with a strong back flow occurring at both sides of the central flow, as depicted in Fig. 2(n–q).

We noted that further increasing the radial index value b as 0.5 will make changes in the input beam structure as shown in Fig. 3(a). The electric field vectors are double focal spots with a spiral structure for both transverse and longitudinal component, which produced double spiral total intensity at the focal plane and are mentioned in Fig. 3(b–d).

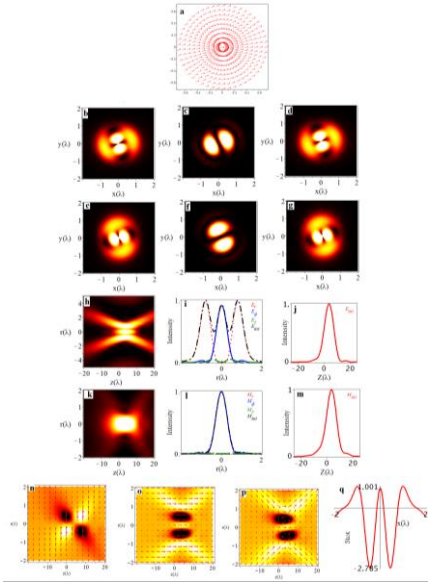

Fig. 2. Electric, magnetic and Poynting vector distribution for b = 0.1 with c = 0.

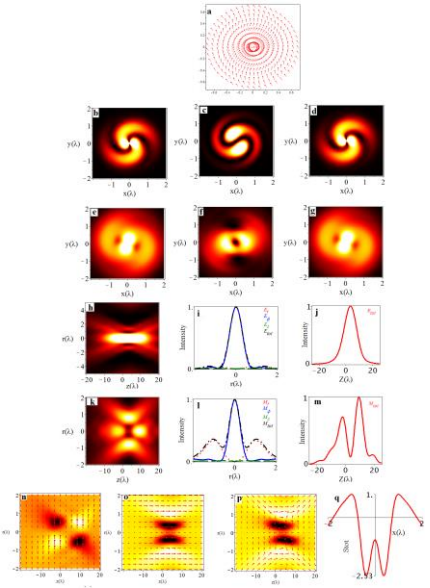

Fig. 3. Electric, magnetic and Poynting vector distribution for b = 0.5 with c = 0.

The magnetic field vector in transverse field got a spiral thimble structure and produced a small cage-like structure in the longitudinal component. The total field is transversely dominated, as mentioned in Fig. 3(e–g).The electric field is *a* optical needle through focus with FWHM of 1λ, DOF of 30λ and the corresponding magnetic field turns to an optical cage-like structure, as shown in Fig. 3(h–m). The longitudinal component of the Poynting vector shows the back flow of energy through focus and the total Poynting vector is the sum of a transverse and longitudinal component as shown in Fig. 3(n–q).

 © 2023 Photonics Society of Poland

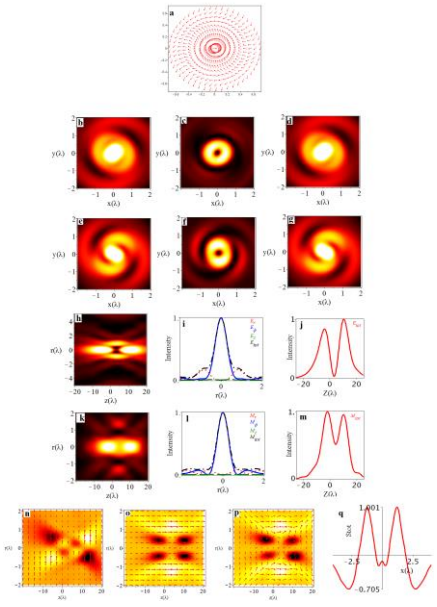

Fig. 4. Electric, magnetic and Poynting vector distribution for b = 1.0 with c = 0.

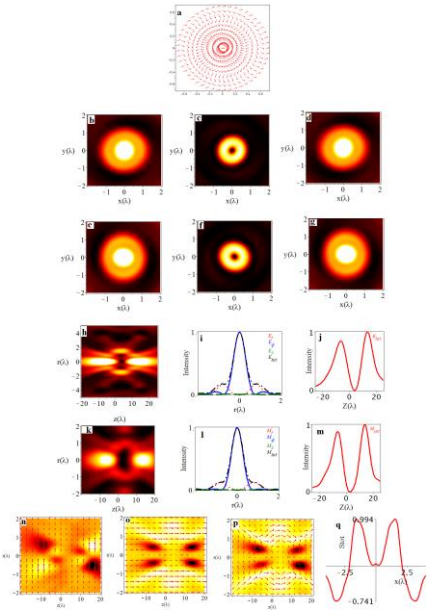

Fig. 5. Electric, magnetic and Poynting vector distribution for b = 1.5 with c = 0.

After increasing the radial component to 1, the input beam also changed radically, as mentioned in Fig. 4(a). The transverse component of the electric field is the hot spot with spirality, whereas the longitudinal component becomes a bubble-like structure with spirality, as shown in Fig. 4(b–d).The magnetic field distribution in the focal plane is the same as the electric field distribution, but a small position change occurs in the intensity distribution, as shown in Fig.4 (e–g). The electric and magnetic field distribution through focus are an optical cage-like structure and splitted focal segment, as shown in Fig. 4(h–m). Both electric and magnetic field distributions are dominated by E_ϕ and M_ϕ components, as shown in Fig. 4(i and l). The transverse Poynting vector component undergoes small changes as compared to the previous cases and, at the same time, the longitudinal Poynting vector component gets a small reverse flow of energy, which is reflected in the total Poynting vector distribution, as shown in Fig. 4(n–q).

Further increasing b to 1.5, the transverse components of electric and magnetic fields are spherical spots with small spirality at the same time, magnetic fields are spherical ring with small spirality which makess spherical spiral spots in the focal plane are described in Fig. 5(b-g). On the other hand, optical cage like structures in both electric and magnetic fields through focus are shown in Fig. 5 (h–m). The electric and magnetic components are only depends by the E_ϕ and M_ϕ respectively. The total Poynting vector distribution is observed to be not having any back flow of energy and are dominated both $S_{r+\phi}$ and S_z, as shown in Fig. 5 (n–q).

In conclusion, we theoretically demonstrate the electric and magnetic energy densities as well as energy flux for radially variant vector beam focusing through a dielectric interface. Based on the theoretical model, we generates novel focal structures for corresponding radial indices. At the same time, the energy flux in the geometrical plane gets forwarded and reversed depends on the radial and azimuthal index value. These peculiar properties can apply the fields such as optical trapping, optical recording, magnetic recording, and magnetic resonance microscopy and semiconductor inspection.

References

[1] S.N. Khonina, I. Golub, Opt. Lett. **36**, 352 (2011).
[2] V.V. Kotlyar *et al.*, Appl. Opt. **52**, 330 (2013).
[3] S. Sen, M.A. Varshney, D. Varshney, ISRN Optics. **2013**, 1 (2013).
[4] M. Martínez-Corral *et al*., Appl. Phys. Lett. **85**, 4319 (2004).
[5] J. Lekner, Opt. A: Pure Appl. Opt. **5**, 6 (2003).
[6] H. Guo *et al*.,Opt. Express 21, 5363 (2013).
[7] C.-C. Sun, C.-K. Liu,Opt. Lett. **28**, 99 (2003).
[8] G.H. Yuan, S.B. Wei, X.-C. Yuan, Opt. Lett. **36**, 3479 (2011).
[9] P. Yu *et al*., Lett. **40**, 3229 (2015).
[10] Z. Chen, T. Zeng, B. Qian, J. Ding, Opt. Expr. **23**, 17701 (2015).
[11] Z. Liu *et al*., Photon. Res. **5**, 15 (2017).
[12] Z. Man *et al*., J. Opt. Soc. Am. A **35**, 1014 (2018).
[13] Z. Man, S. Fu, G. Wei, J. Opt. Soc. Am. A **34**, 1384 (2017).
[14] Z. Man *et al*., Appl. Opt. **57** (2018).
[15] S.S. Stafeev *et al*., IEEE Photon. J., **11**, 1 (2019).
[16] S.S. Stafeev, V.V. Kotlyar, Opt. Commun. **450**, 67 (2019).
[17] S.S. Stafeev *et al*., Proc. SPIE **11025**, 1102518 (2019).
[18] N.G. Orji, M. Badaroglu, B.M. Barnes, Nat. Electron. **1**, 532 (2018).
[19] P. Torok, P. Varga, G.R. Booker, J. Opt. Soc. Am. A **12**, 2136 (1995).
[20] P. Torok *et al*., J. Opt. Soc. Am. A **12**, 325 (1995).
[21] Z. Zhou, L. Zhu, Optik **124**, 2219 (2013).
[22] J. Shu, Z. Chen, J. Pu, Y. Liu, J. Opt. Soc. Am. A **31**, 1180 (2014).
[23] K. Hu, Z. Chen, J. Pu., Opt. Lett. **37**, 3303 (2012).
[24] B. Richards, E. Wolf, Proc. R. Soc. London A **253**, 358 (1959).

 © 2023 Photonics Society of Poland